

## Resistive Wall Instability in the KEK 12GeV PS

T. Toyama, D. Arakawa, S. Igarashi, J. Kishiro, K. Takayama  
 High Energy Accelerator Research Organization (KEK)  
 1-1 Oho, Tsukuba, Ibaraki 305 Japan

### Abstract

Investigation of the beam loss at the beginning of acceleration clarified the loss mechanism due to the horizontal head-tail instability. The instability occurs due to a large change in the chromaticity produced by the sextupole field induced in the beam-pipe of the dipole magnets. The horizontal chromaticity increases up to a positive value just around 80 ms after the beginning of acceleration. The longitudinal mode 0, 1 and 2 have been observed. The impedance model explains the instability very well.

### 1 INTRODUCTION

The operating point,  $(\nu_x, \nu_y)$ , has been changed from (7.12, 7.21) to (7.12, 5.21) since January 1996, expecting a reduction of the space-charge induced effects[1]. After the modification, the beam loss emerges around 80 ms after the beginning of acceleration (P2). Chromaticity control using one of the two sextupole families has been the most effective cure to suppress the beam loss. The observation using the position monitor revealed that the instability is caused by a horizontal coherent dipole motion, which was identified as the Head-Tail Instability (HTI) of longitudinal mode, mainly,  $\ell = 0$ . The beam loss around 80 ms after P2 has almost vanished by properly exciting sextupoles.

In this paper observed phenomena and its analysis using the Sacherer's formula are presented.

### 2 EXPERIMENTAL RESULTS

The typical profile of the horizontal coherent dipole oscillation is shown in Fig.1. In Fig.2 the growth of the oscillation is shown in the lower trace and the degradation of a beam intensity in the upper trace. The signals are sampled at the timing of the bunch center, 5 k samples per division. The start point of the trace is 50 ms after P2. The instabilities occur repeatedly even decreasing beam intensity. Around 80 ms from P2 the mode  $\ell = 0$  was mostly observed. On the other hand the mode  $\ell = 1, 2$  or some mixtures were observed at the neighbour of the above time region.

It is well known that the head-tail motion of mode  $\ell = 0$  is unstable in the positive chromaticity region under the transition energy and has no instability threshold in the beam intensity[2][3].

Near injection energy, there are some contributions to the chromaticity other than natural chromaticity, [4]: an excitation of two families of correction sex-

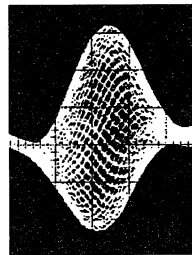


Figure 1: Horizontal coherent oscillation.

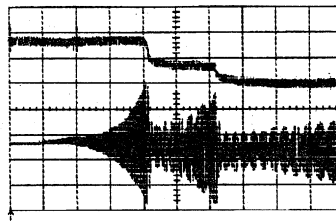


Figure 2: Growth of the coherent oscillation. Upper trace: beam intensity ( $10^{11}$  protons/div), lower trace: coherent oscillation, abscissa: 5 k samples/div.

tupoles ( $\Delta\xi_{x\ sext}$ ), a remnant of the correction sextupoles ( $\Delta\xi_{x\ remnant}$ ), a sextupole component of the dipole and quadrupole magnets ( $\Delta\xi_{x\ di}$ ,  $\Delta\xi_{x\ quad}$ ), and an eddy current in the dipole beam-pipe ( $\Delta\xi_{x\ eddy}$ ). Taking the energy dependence of the chromaticity into account as

$$\xi_x(t) = \xi_{x\ natural} + \Delta\xi_{x\ sext} + \Delta\xi_{x\ di} + \Delta\xi_{x\ quad} + \Delta\xi_{x\ remnant} \frac{B(0ms)}{B(t)} + \Delta\xi_{x\ eddy} \frac{\dot{B}(t)/B(t)}{\dot{B}(100ms)/B(100ms)}$$

we obtain the time evolution of the chromaticity, which is shown with the measured chromaticity in Fig.3. The solid line and the filled circles are the calculated and measured results, respectively, for the operation in which the beam loss occurs due to the uncorrected chromaticity at (7.12, 5.21). The calculation including the eddy current effect well agrees with the measured result and well explains the beam loss around 80 ms from P2, when the chromaticity takes the positive value around 80 ms from P2.

The natural chromaticity is  $\xi_x = -9.22$  for the previous operating point, (7.12, 7.21). After reducing the vertical tune, the natural chromaticity increased by  $\sim 1.3$ , became closer to zero. This caused zero crossing of the horizontal chromaticity around 80 ms after P2 and forced the horizontal coherent motion, mainly, of mode 0 unstable and resulted in the beam loss.

Since the incoherent space charge tune shift has no

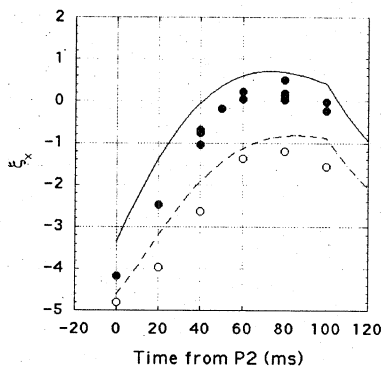


Figure 3: Horizontal chromaticity after the acceleration start.

effect for the transverse dipole mode, we need some other stabilizing effects. The cure has been achieved by the defocusing sextupole family ( $S_D$ ) because of the power supply polarity. Corresponding chromaticities are plotted in Fig.3 by the dashed line (calculated result) and the open circles (measured result).

In order to fully understand the feature of the instability, including modeling of coupling impedances, and to investigate most proper cure, the growth rate was measured with various conditions.

Measured growth rate as a function of the chromaticity with single bunch is depicted in Fig.4. Because the measurement was made during acceleration, the growth rate is normalized by the revolution frequency  $\omega_0$ .

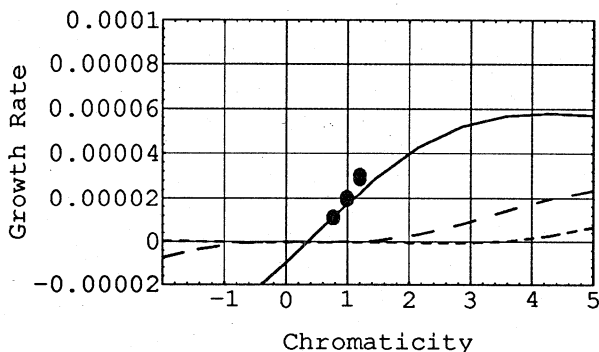


Figure 4: Growth rate as a function of horizontal chromaticity.

The measured growth rate as a function of the bunch intensity was depicted in Fig.5.

### 3 ANALYSIS

The qualitative feature of the observed HTI was well explained by a multi-particle simulation code, although a constant wake was used.[4]

In order to obtain more quantitative feature, the growth rate is calculated using the Sacherer's formula[2][3][5] along with an impedance model.

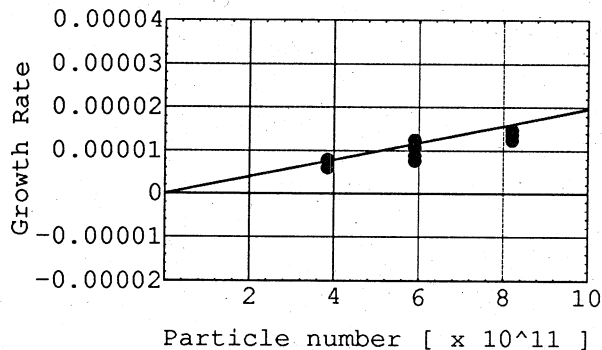


Figure 5: Growth rate as a function of bunch intensity.

Table 1: Beam and machine parameters

$\omega_0$	$2\pi \times 7.67$ kHz
$\omega_s$	$2\pi \times 4$ kHz
$N_b$	$5.8 \times 10^{11}$ protons/bunch
$\nu_x$	7.15
$\tau_b$	75 ns
$E$	700 + 938 MeV
$\eta$	-0.22

The growth rate normalized by  $\omega_0$  is

$$\text{Im}[\Delta\nu_\ell^\perp],$$

where

$$\Delta\nu_\ell^\perp = \frac{-i}{\ell + 1} \frac{ecN_b}{4\pi\nu_x\omega_0\tau_b E/e} \frac{\sum_{p=-\infty}^{+\infty} Z_\perp(\omega_p^\perp) h_m(\omega_p^\perp - \omega_\xi)}{\sum_{p=-\infty}^{+\infty} h_m(\omega_p^\perp - \omega_\xi)},$$

$$\omega_p^\perp = (p + \nu_x)\omega_0 + \ell\omega_s,$$

$p$ =integer,  $\ell$  is the azimuthal mode number,  $\omega_0$  the revolution frequency,  $\omega_s$  the synchrotron frequency,  $e$  the electron charge,  $c$  the light speed,  $N_b$  the bunch intensity,  $\nu_x$  the horizontal tune,  $\tau_b$  the total bunch length,  $E$  the total energy,  $\omega_\xi = \xi/\eta$  the chromatic frequency, and  $\eta$  the slippage factor. The parameters used for the calculation are summarized in Table 1.

For coupling impedances a resistive wall impedance, a kicker impedance and a broad band impedance are assumed. The resistive wall is considered to comprise two parts, one from almost rectangular beam pipes[6] in the bends and quads ( $Z_{RW\perp}^{(m)}$ ) and one from almost cylindrical beam pipes in straight sections ( $Z_{RW\perp}^{(s)}$ ), i.e.

$$Z_{RW\perp}^{(m)} \approx (\text{sgn}(w) - i) \frac{R_{(m)}}{b_{(m)}^3} \frac{\pi^2}{24} \sqrt{\frac{2\rho}{\epsilon_0|\omega|}},$$

Table 2: Parameters for the resistive wall impedance

$R_{(m)}$	200 m
$R_{(s)}$	140 m
$b_{(m)}$	25.5 mm
$b_{(s)}$	60 mm
$\rho$	$9 \times 10^{-7} \Omega\text{m}$

Table 3: Kicker parameters (for one module)

$Z_s$	377 $\Omega$
$Z_0$	25 $\Omega$
$a$	25 mm
$b$	62.5 mm
$v_{kicker}/c$	0.028
$v_{cable}/c$	0.67
$l_{(k)}$	250 mm
$l'_{(k)}$	55 m

and

$$Z_{RW\perp}^{(s)} \approx (sgn(w) - i) \frac{R_{(s)}}{b_{(s)}^3} \sqrt{\frac{2\rho}{\epsilon_0|\omega|}},$$

where  $2\pi R_{(m)}$  and  $2\pi R_{(s)}$  are the total length of the magnet section and the straight section, respectively,  $\rho$  the vacuum chamber resistivity,  $b_{(m)}$  the half height of the beam pipe and  $b_{(s)}$  the pipe radius. The relevant parameters are summarized in Table 2.

There are five identical kickers in the 12GeV PS. Its impedance (real part) is [7]

$$Re[Z_{\perp}^{(k)}] = \frac{Z_{T0} [sin(kl_k) + tan(k'l'_k)cos(kl_k) - tan(k'l'_k)]^2}{kl_k (1 + tan^2(k'l'_k))},$$

where  $a$  and  $b$  are the half height and the half width of the kicker aperture,  $Z_{T0} = Z_s l_k / (4ab)$ ,  $k = \omega / v_{kicker}$ ,  $k' = \omega / v_{cable}$ ,  $l_k$  and  $l'_k$  the length of the kicker and cable, respectively,  $Z_s$  is the vacuum impedance,  $v_{kicker} = Z_0 a / (\mu_0 b)$  velocity in the kicker,  $v_{cable}$  velocity in the cable and  $Z_0$  is the characteristic impedance of the kicker. Each kicker is matched at one end and connected with a cable at the other end which is approximately open at the end of the cable. The parameters used in the calculation are summarized in Table 3.

For the broad band impedance

$$Z_{BBL} = \frac{\omega_r}{\omega} \frac{R_T}{1 + iQ(\omega_r/\omega - \omega/\omega_r)},$$

the following parameters are assumed.[5]

Table 4: Broad band impedance

$R_T$	3 M $\Omega$ /m
$\omega_r$	$2\pi \times 1.4$ GHz
$Q$	1

The form factor,  $h_m(\omega)$  for parabolic distribution is

$$h_\ell(\omega) = (\ell + 1)^2 \frac{1 + (-1)^\ell \cos(\omega\tau_b)}{[(\omega\tau_b/\pi) - (\ell + 1)^2]^2}.$$

The calculated results are depicted in Fig.4 and Fig.5. In Fig.4 the growth rate for the mode  $\ell = 0, 1$  and 2 are plotted by a solid line, a dashed line and a dotted line, respectively. These results agree with the measured values very well. It should be noted that three impedances contribute almost equally to the growth rate.

#### 4 SUMMARY

The observed feature of the HTI is well explained by the Sacherer's theory and the present impedance model.

We are further investigating the HTI, which comprises single- and multi-bunch effects, and will optimize the cure.

#### 5 ACKNOWLEDGEMENTS

The authors wish to thank KEK-PS members for their interest and continual support through this work. They wish to thank Prof. I. Yamane and Prof. H. Sato for calling their attention to the present problem. They also wish to thank Dr. M. Shirakata, Dr. M. Uota and Miss K. Koba for helping in the experiment and giving usefull comments.

#### 6 REFERENCES

- [1] S. Machida and Y. Shoji, AIP Conf. Proc. 377 (1995) p.160, S. Machida, Nucl. Instr. Meth. A 384 (1997) 316. and Y. Shoji et al., submitted to the 1997 Part. Accel. Conf., May 12-16, 1997, Vancouver, BC, Canada.
- [2] B. Zotter and F. Sacherer, CERN 77-13, p.175.
- [3] A. Chao, "Physics of collective beam instabilities in high energy accelerators", John Wiley & Sons, Inc., 1993 and the references there in.
- [4] T. Toyama et al., submitted to the 1997 Part. Accel. Conf., May 12-16, 1997, Vancouver, BC, Canada.
- [5] R. Cappi, Part. Accel. 50 (1995) 117.
- [6] K. Y. Ng, Part. Accel. 16 (1984) 63.
- [7] G. Nassibian, CERN/PS 85-68 (BR), 1986.